

From antiferromagnetic order to magnetic textures in the two dimensional Fermi Hubbard model with synthetic spin orbit interaction

Jiří Minář

Centre for Quantum Technologies, National University of Singapore, Singapore

Benoît Grémaud

Centre for Quantum Technologies, National University of Singapore, Singapore

Department of Physics, National University of Singapore, Singapore and

Laboratoire Kastler Brossel, Ecole Normale Supérieure CNRS, UPMC; 4 Place Jussieu, 75005 Paris, France

We study the interacting Fermi-Hubbard model in two spatial dimensions with synthetic gauge coupling of the spin orbit Rashba type, at half-filling. Using real space mean field theory, we numerically determine the phase as a function of the interaction strength for different values of the gauge field parameters. For a fixed value of the gauge field, we observe that when the strength of the repulsive interaction is increased, the system enters into an antiferromagnetic phase, then undergoes a first order phase transition to a non collinear magnetic phase. Depending on the gauge field parameter, this phase further evolves to the one predicted from the effective Heisenberg model obtained in the limit of large interaction strength. We explain the presence of the antiferromagnetic phase at small interaction from the computation of the spin-spin susceptibility which displays a divergence at low temperatures for the antiferromagnetic ordering. We discuss, how the divergence is related to the nature of the underlying Fermi surfaces. Finally, the fact that the first order phase transitions for different gauge field parameters occur at unrelated critical interaction strengths arises from a Hofstadter-like situation, i.e. for different magnetic phases, the mean-field Hamiltonians have different translational symmetries.

PACS numbers: 67.85. d 05.30.Fk 37.10.Jk 71.70.Ej

I. INTRODUCTION

The recent progress of experiments using cold atomic gases^{1–3}, in particular in implementing artificial gauge fields^{4–10}, has open the door to the studies of a whole class of model Hamiltonians, some directly inherited from condensed matter physics (quantum Hall effects), but, more saliently, some are genuinely generating new physical situations, allowing physicists to further develop and test theoretical ideas, like topological phases^{11,12}, non-abelian particles¹³ or mixed dimensional systems^{14–18}. In particular, the experiments involving spinors, made of either bosons or fermions in different Zeeman sub-levels, are now able to produce non-abelian gauge-fields, leading to a kinetic term allowing for a modification of the internal degrees of freedom along the propagation of the particle¹⁹. In two-dimensional lattices, the non-abelian gauge fields result in tight-binding Hubbard models with spin-flip hopping terms, i.e. the hopping matrices are not diagonal anymore in the spin degrees of freedom. Among all the possibilities, an artificial gauge-field mimicking a spin-orbit coupling term¹⁹ (see below) is probably the most well-known and studied situation, for two reasons: (i) it corresponds to a spatially independent vector potential leading to relatively simple analytical treatment, especially in the bulk situation; (ii) it leads to highly non-trivial features like broken time-reversal ground states and/or magnetic textures with topological properties, like skyrmion crystal^{20,21}.

The cases of two components bosons or fermions in the presence of a spin-orbit coupling have been the objects

of recent analytical and numerical studies^{20–26}. In particular, in the case of repulsive interactions, they have emphasized various magnetic ordering and textures depicted by the effective spins. One must note that in the large interaction strength, and close to half-filling, both bosonic and fermionic situations can be described by effective and quite similar Heisenberg models involving the spin degrees of freedom only (see below). The case of fermions with attractive interaction has also been studied, emphasizing the impact of the spin-flip terms on the pairing states, like the BCS-BEC crossover or the Fulde-Ferrel-Larkin-Ovchinnikov (FFLO) phase^{27–32}. The instabilities of attracting bosons with such a spin-orbit coupling have also been considered³³.

Even though the Bose-Hubbard model and the Fermi-Hubbard model with a spin-orbit coupling depicts similar phases in the strong (repulsive) interaction limit, the behavior for small coupling is obviously different: the Mott regime of the bosonic models turns into a complex superfluid regime whereas fermionic models are expected to be in a Mott insulator state. Still, in the later case, the evolution of the magnetic ordering from the non-interacting situation towards the Heisenberg model regime remains largely unexplored. In the present paper, using both a linear response approach and real space mean-field theory, we emphasize that the Fermi-Hubbard model at half-filling, in the presence of a spin-orbit coupling, still depicts, at low interaction, an antiferromagnetic phase, corresponding to the Fermi-Hubbard model *without* spin-orbit coupling. The impact of the gauge-field then results, at intermediate interaction depending

on the strength of the spin-orbit coupling, in a first order phase transition towards a non collinear magnetic order, which further evolves to magnetic texture at large interaction, predicted by the effective Heisenberg model.

The paper consists in two main parts: in Section II, we describe the theoretical framework (Fermi-Hubbard model, linear response theory, effective Heisenberg model). In Section III (i) we show that the non-interacting energies (band structure) always depict a nesting at the antiferromagnetic order resulting in a diverging spin-spin susceptibility at low temperature and, thereby, an instability towards an antiferromagnetic phase at small interaction; (ii) we provide the numerical mean-field results for different values of the spin-orbit coupling and the interaction, showing evidences for the transition from the antiferromagnetic order to a non-collinear magnetic order. In particular, the skyrmionic phase is shown to already exist for moderate values of the interaction.

II. METHODS

A. model

In this paper we consider a system of spin 1/2 fermionic particles in 2D square lattice and subjected to a synthetic gauge field (more will be said about the specific form of the gauge field later). The lattice spacing is equal to unity, setting both spatial and momentum scales. The system Hamiltonian reads

$$H_{\text{tot}} = H_{\text{kin}} + H_{\mu} + H_{\text{int}}, \quad (1)$$

where

$$H_{\text{kin}} = - \sum_{\mathbf{j}, \mathbf{j}'} c_{\mathbf{j}, s}^{\dagger} T_{\mathbf{j}, \mathbf{j}'}^{s, s'} c_{\mathbf{j}', s'} \quad (2a)$$

$$H_{\mu} = - \sum_{\mathbf{j}} \mu_1 n_{\mathbf{j}, 1} + \mu_2 n_{\mathbf{j}, 2} \quad (2b)$$

$$H_{\text{int}} = U \sum_{\mathbf{j}} \left(n_{\mathbf{j}, 1} - \frac{1}{2} \right) \left(n_{\mathbf{j}, 2} - \frac{1}{2} \right), \quad (2c)$$

where T are the tunneling matrices and are taken to be time independent in the following. $c_{\mathbf{j}, s}^{\dagger}, c_{\mathbf{j}', s'}$ are the usual fermionic creation and annihilation operators satisfying $\{c_{\mathbf{j}, s}, c_{\mathbf{j}', s'}^{\dagger}\} = \delta_{\mathbf{j}, \mathbf{j}'} \delta_{s, s'}$, $n_{\mathbf{j}, s} = c_{\mathbf{j}, s}^{\dagger} c_{\mathbf{j}, s}$ is the density operator, μ_s the chemical potential, U the interaction strength and $s = 1, 2$ labels the spin degree of freedom. The interaction Hamiltonian can be written also as

$$H_{\text{int}} = - \frac{2U}{3} \sum_{\mathbf{j}} \mathbf{S}_{\mathbf{j}} \cdot \mathbf{S}_{\mathbf{j}}, \quad (3)$$

where $S_{\mathbf{j}}^a = \frac{1}{2} c_{\mathbf{j}, s}^{\dagger} \sigma_{s, s'}^a c_{\mathbf{j}, s'}$ are the usual spin operators.

To be more specific, when needed, we will consider the case of the gauge fields corresponding to the spin-orbit

coupling of the Rashba type, corresponding to the position independent tunnelling in the x and y directions:

$$T_x = t e^{-i\alpha\sigma_y} = t \begin{pmatrix} \cos(\alpha) & -\sin(\alpha) \\ \sin(\alpha) & \cos(\alpha) \end{pmatrix} \quad (4a)$$

$$T_y = t e^{i\alpha\sigma_x} = t \begin{pmatrix} \cos(\alpha) & i \sin(\alpha) \\ i \sin(\alpha) & \cos(\alpha) \end{pmatrix}. \quad (4b)$$

where t denotes the global strength of the hopping amplitudes and we have used the labelling $T_x = T_{\mathbf{j}, \mathbf{j}+1_x}$ and $T_y = T_{\mathbf{j}, \mathbf{j}+1_y}$.

B. Non-interacting case - $U = 0$

In the case where the matrices $T_{\mathbf{j}, \mathbf{j}'}$ are position independent, the Hamiltonian Eq.(2a) + Eq.(2b) is diagonalized in the momentum space:

$$H_0 = - \sum_{\mathbf{k}} C_{\mathbf{k}}^{\dagger} \mathcal{T}_{\mathbf{k}} C_{\mathbf{k}}, \quad (5)$$

where $C_{\mathbf{k}}^{\dagger} = (c_{\mathbf{k}, 1}^{\dagger}, c_{\mathbf{k}, 2}^{\dagger})$ and

$$\mathcal{T}_{\mathbf{k}} = (T_x e^{-ik_x} + T_x^{\dagger} e^{ik_x} + T_y e^{-ik_y} + T_y^{\dagger} e^{ik_y} + \hat{\mu})$$

$$\hat{\mu} = \begin{pmatrix} \mu_1 & 0 \\ 0 & \mu_2 \end{pmatrix}. \quad (6)$$

Finally, the matrix $\mathcal{T}_{\mathbf{k}}$ is diagonalized with a unitary matrix $U_{\mathbf{k}}$, such that

$$H_0 = \sum_{\mathbf{k}, s} \epsilon_{\mathbf{k}, s} d_{\mathbf{k}, s}^{\dagger} d_{\mathbf{k}, s}, \quad (7)$$

where $(d_{\mathbf{k}, 1}^{\dagger}, d_{\mathbf{k}, 2}^{\dagger}) = (c_{\mathbf{k}, 1}^{\dagger}, c_{\mathbf{k}, 2}^{\dagger}) U_{\mathbf{k}}^{\dagger}$.

In the specific case of the spin-orbit coupling (4), one obtains the following eigenenergies:

$$\epsilon_{\mathbf{k}, 1, 2} = -\mu - 2t \left[(\cos k_x + \cos k_y) \cos \alpha \right. \\ \left. \pm \sqrt{(\sin^2 k_x + \sin^2 k_y) \sin^2 \alpha + h^2} \right], \quad (8)$$

where μ is the chemical potential and h is the spin imbalance defined through $\mu_{1, 2} = \mu \pm h$ (see Eq.(6)). The situation gets simpler in the limit of $\mu = h = 0$, which corresponds to half filling for all α .

C. Linear Response in small U limit

Turning on the interaction, one expects the Fermi liquid phase to be unstable towards a magnetically ordered phase. This instability of the system can be captured using the standard linear response theory (see Appendix A for details), more precisely from the spin-spin susceptibility. Let us start with the non interacting Hamiltonian of the form

$$H = H_0 + H_{\text{ext}},$$

where H_0 is given by Eq.(5) and

$$H_{\text{ext}} = \sum_{\mathbf{j}} S_{\mathbf{j}}^a B_{\mathbf{j}}^a(t) = \frac{1}{N} \sum_{\mathbf{q}} S_{-\mathbf{q}}^a B_{\mathbf{q}}^a(t),$$

where B is the external driving force. Using the Fourier transform of the fermionic operators $c_{\mathbf{k},s} = \frac{1}{\sqrt{N}} \sum_{\mathbf{j}} e^{-i\mathbf{k}\cdot\mathbf{j}} c_{\mathbf{j},s}$, where N is the number of sites, one gets $S_{\mathbf{j}}^a = \frac{1}{N} \sum_{\mathbf{q}} e^{i\mathbf{q}\cdot\mathbf{j}} S_{\mathbf{q}}^a$ and $S_{\mathbf{q}}^a = \frac{1}{2} \sum_{\mathbf{k}} c_{\mathbf{k},s}^\dagger \sigma_{s,s'}^a c_{\mathbf{k}+\mathbf{q},s'}$.

The spin-spin susceptibility is diagonal in the momentum space and reads

$$\chi_{\mathbf{q}}^{a,b}(\omega) = -i \int_0^{+\infty} d\tau e^{-i\omega\tau} \langle [S_{\mathbf{q}}^a(\tau), S_{-\mathbf{q}}^b(0)] \rangle, \quad (9)$$

where the thermal average and the time evolution are done using the unperturbed Hamiltonian H_0 . Therefore, the analytic expression for the susceptibility is easily obtained by diagonalizing H_0 . After some manipulation, we find, that

$$\begin{aligned} \chi_{\mathbf{q}}^{a,b}(\omega) &= \frac{1}{N} \sum_{\mathbf{k},s,s'} (S_{\mathbf{k},\mathbf{k}+\mathbf{q}}^a)_{s,s'} (S_{\mathbf{k}+\mathbf{q},\mathbf{k}}^b)_{s',s} \frac{n(\epsilon_{\mathbf{k},s'}) - n(\epsilon_{\mathbf{k}+\mathbf{q},s})}{\omega + \epsilon_{\mathbf{k},s'} - \epsilon_{\mathbf{k}+\mathbf{q},s} + i\eta} \\ &\rightarrow \frac{1}{(2\pi)^2} \int d^2k \sum_{s,s'} (S_{\mathbf{k},\mathbf{k}+\mathbf{q}}^a)_{s,s'} (S_{\mathbf{k}+\mathbf{q},\mathbf{k}}^b)_{s',s} F_{s,s'}(\omega, \mathbf{k}, \mathbf{q}), \end{aligned} \quad (10)$$

where $n(\epsilon) = (1 + e^{\beta\epsilon})^{-1}$ is the Fermi function. We have introduced

$$F_{s,s'}(\omega, \mathbf{k}, \mathbf{q}) = \frac{n(\epsilon_{\mathbf{k},s'}) - n(\epsilon_{\mathbf{k}+\mathbf{q},s})}{\omega + \epsilon_{\mathbf{k},s'} - \epsilon_{\mathbf{k}+\mathbf{q},s} + i\eta} \quad (11)$$

and

$$S_{\mathbf{k},\mathbf{k}+\mathbf{q}}^a = \frac{1}{2} U_{\mathbf{k}} \sigma^a U_{\mathbf{k}+\mathbf{q}}^\dagger, \quad (12)$$

where η is an infinitesimal convergence factor. In the usual situation of a Hamiltonian diagonal in the original spin-space, the matrices $U_{\mathbf{k}}$ are simply the identity and one recovers the standard spin-spin susceptibility.

In what precedes, we have derived the susceptibility Eq.(10) for the non-interacting system. However, the interaction among the fermions affects the spin-spin susceptibility. This can be captured, in the random phase approximation (RPA) framework, by deriving, in a self-consistent way, the effective propagator for the spin fluctuations. This is equivalent to perform a mean-field approximation to the interacting Hamiltonian^{35–37}.

Lets recall the main step: Starting from the interaction Hamiltonian Eq.(3), the effect of interaction then

amounts to an introduction of an effective driving force given by

$$H_{\text{ext}}^{\text{eff}} = H_{\text{ext}} + H_{\text{int}}^{\text{MF}} = \sum_{\mathbf{q}} S_{-\mathbf{q}}^b(t) (B_{\mathbf{q}}^b)^{\text{eff}}(t), \quad (13)$$

where $(B_{\mathbf{q}}^b)^{\text{eff}}(t) = [B_{\mathbf{q}}^b(t) - 2g\langle S_{\mathbf{q}}^b(t) \rangle]$ and we have introduced $g = 2U/3$ (see Appendix A). After the manipulation described in Appendix A one finds the expression for average values of the spin operators

$$\langle \mathbf{S}_{\mathbf{q}} \rangle(\omega) = M_{\mathbf{q}}^{-1}(\omega) \chi_{\mathbf{q}}(\omega) \mathbf{B}_{\mathbf{q}}(\omega) \quad (14)$$

where $M_{\mathbf{q}}^{ab}(\omega) = \delta^{a,b} + 2g\chi_{\mathbf{q}}^{a,b}(\omega)$. $M_{\mathbf{q}}^{-1}(\omega)\chi_{\mathbf{q}}(\omega)$ is therefore the RPA susceptibility, whose singularities in the complex ω plane correspond to the vanishing eigenvalues of $M_{\mathbf{q}}(\omega)$.

D. Large U limit - the Heisenberg Hamiltonian

Following the method of³⁴, one obtains, in the large (repulsive) interaction U limit and at half-filling, the following effective Heisenberg Hamiltonian, up to the second order in the t/U expansion:

$$H = H_c + \sum_{\delta=x,y} \sum_{\langle i,i+\delta \rangle} \sum_{a=x,y,z} J_{\delta}^a S_i^a S_{i+\delta}^a + \mathbf{D}_{\delta+} \cdot (\mathbf{S}_i \times \mathbf{S}_{i+\delta})_+ + \mathbf{D}_{\delta-} \cdot (\mathbf{S}_i \times \mathbf{S}_{i+\delta})_-, \quad (15)$$

where

$$\begin{aligned} (\mathbf{S}_i \times \mathbf{S}_{i+\delta})_+ &= (S_1^y S_2^z, S_1^z S_2^x, S_1^x S_2^y) \\ (\mathbf{S}_i \times \mathbf{S}_{i+\delta})_- &= -(S_1^z S_2^y, S_1^x S_2^z, S_1^y S_2^x) \end{aligned}$$

are the "positive" and "negative" part of the vector product. In the most general case, the coefficients J_{δ}^a , D_{δ}^p and H_c , $\delta = x, y$, $a = x, y, z$, $p = 1, 2, 3$, are quadratic functions of elements of the tunnelling matrices T . The gen-

eral expression can be found in the appendix B. However, the situation will simplify considerably when considering a specific case of spin orbit coupling of Rashba type, see Eq. (4):

$$\begin{aligned} J_\delta^x &= 4\lambda \cos(2\alpha) \\ J_\delta^y &= 4\lambda \\ J_\delta^z &= 4\lambda \cos(2\alpha) \end{aligned}$$

for both spatial directions $\delta = x, y$,

$$\begin{aligned} D_{\delta+}^x &= D_{\delta-}^x = 0 \\ D_{\delta+}^y &= D_{\delta-}^y = -4\lambda \sin(2\alpha) \\ D_{\delta+}^z &= D_{\delta-}^z = 0 \end{aligned}$$

for $\delta = x$ (tunnelling T_x) and

$$\begin{aligned} D_{\delta+}^x &= D_{\delta-}^x = -4\lambda \sin(2\alpha) \\ D_{\delta+}^y &= D_{\delta-}^y = 0 \\ D_{\delta+}^z &= D_{\delta-}^z = 0 \end{aligned}$$

for $\delta = y$, (the tunnelling T_y),

$$H_c = -4\lambda \frac{\mathbb{1}}{4},$$

$\lambda = t^2/U$. This Hamiltonian is identical with Eq. (2) of²⁰, where one has to set their parameter $\lambda = 1$. In the following, we take t equal to unity to set the energy scale.

III. RESULTS & DISCUSSION

A. Small U limit

Here, we study the small interaction behaviour of the lattice gas at half-filling, $\mu = h = 0$, by means of the susceptibility, given by Eq.(10). The instability of the non-interacting ground state is signalled by a divergence of the DC ($\omega = 0$) RPA susceptibility (14), corresponding to a vanishing eigenvalue of $M_{\mathbf{q}}(0)$. The latter corresponds to an eigenvalue of $\chi_{\mathbf{q}}(0)$ having the value $-1/2g$. In the following, we evaluate the susceptibility by numerical integration of (10) over the first Brillouin zone. We will discuss the general \mathbf{q} value below, but it turns out that the mean-field simulations indicate the onset of AF phase for small couplings U , corresponding to a value of $\mathbf{q} = \mathbf{q}_\pi = (\pm\pi, \pm\pi)$. For this specific value of $\mathbf{q} = \mathbf{q}_\pi$, one can see, using Eq.(8), that $\epsilon_{\mathbf{k}+\mathbf{q}_\pi, s} = -\epsilon_{\mathbf{k}, \bar{s}}$, where \bar{s} means the opposite spin to s . Moreover, in this case, the Fermi energy is $E_F = 0$ and one gets nested Fermi surfaces for any value of the gauge field parameter α - the Fermi surfaces together with the susceptibility integrand function $F_{s,s'}(0, \mathbf{k}, (\pi, \pi))$, Eq.(11), are plotted in Fig.(1) for different values of α . The coincidence of the maximum of the integrand function F is a specific feature of

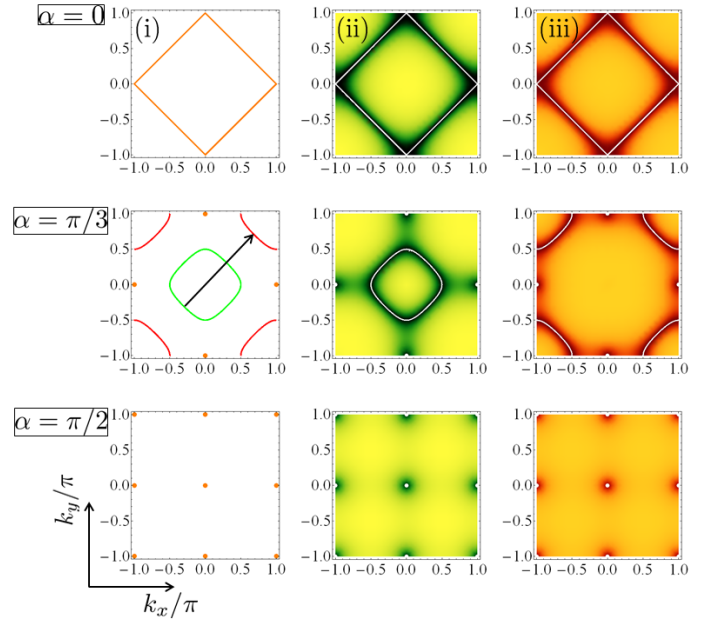


FIG. 1. (Color online) Plots of Fermi surfaces and susceptibility integrand F (see Eq.(11)) in the first BZ for $\mathbf{q} = (\pi, \pi)$. Rows: successive values of $\alpha = 0, \pi/3, \pi/2$; Columns: (i) Fermi surfaces. The nesting of Fermi surfaces is indicated explicitly for $\alpha = \pi/3$. For $\alpha = \pi/2$ the Fermi surface becomes a set of isolated Dirac points. (ii) F for spins $(s, s') = (2, 1)$, (iii) F for spins $(s, s') = (1, 2)$. The green and red colours in (ii) and (iii) represent the maximum of F . The Fermi surfaces for given (s, s') in (ii) and (iii) are indicated by white lines. The coincidence of Fermi surfaces and the maximum of the integrand F is not generic, but is specific for $\mathbf{q}_\pi = (\pm\pi, \pm\pi)$.

\mathbf{q}_π and is responsible for the the onset of AF phase for sufficiently low temperature, i.e. large β values. Indeed, we note, that in the case of nested Fermi surfaces, the susceptibility possess $\ln\beta$ divergence.

Moreover, for $\alpha = 0$, the presence of Van Hove singularities at the Fermi energy adds a leading divergence $\ln^2\beta$. Therefore, we fit the susceptibility with a function

$$\chi_{\text{fit}} = a \ln^2 \beta + b \ln \beta + c. \quad (16)$$

The results are summarized in Table I and plotted in Fig.(2). With respect to the preceding discussion, one can distinguish two cases - $\alpha = 0$ and $\alpha > 0$. We verified, that for $\alpha = 0$, our results agree with the theoretical prediction given by Eq.(7) in^{38,39} (first two lines in Table I)

$$\chi_{\mathbf{q}_\pi, \text{theor}} = -\frac{1}{2\pi^2 \bar{t}} \ln^2 \frac{16e^{\gamma} \bar{t}}{\pi} \beta + C_0. \quad (17)$$

For $\alpha > 0$ (α strictly positive), the absolute value of b decreases monotonically as the nesting of Fermi surfaces decreases. Also, for $\alpha > 0$ the a term becomes significantly smaller than for the $\alpha = 0$ case (no $\ln^2 \beta$ divergence).

α	$a \times 10^3$	b	c	$\sigma^2 \times 10^6$
0 (theor)	-13.	-0.073	-0.098	120.
0 (fit)	-13.	-0.073	-0.1	0.73
0.05	3.	-0.13	-0.057	6.6
$\pi/12$	0.9	-0.065	-0.11	2.
$\pi/6$	0.38	-0.043	-0.1	2.7
$\pi/4$	-0.76	-0.025	-0.1	1.6
$\pi/3$	-0.68	-0.016	-0.088	0.032
$5\pi/12$	-0.85	-0.0052	-0.082	1.6
$\pi/2$	-0.95	0.0047	-0.084	1.4

TABLE I. Values of the fitting parameters a, b, c of Eq.(16) for different values of the gauge field parameter α . σ^2 is the usual data variance, defined in the text. The first line corresponds to the theoretical prediction Eq.(17) and agrees well with the numerical computation of the susceptibility Eq.(10) shown in the second line.

The data variance in the Table I reads $\sigma^2 = \frac{1}{n} \sum_{i=1}^n |\chi_{\text{fit},i} - \chi_i|^2$, where χ_i stands for a minimal eigenvalue at (given) \mathbf{q}_π and $n = 14$ is the number of simulated data points. As shown in Fig.(2), the parameter of the $\ln\beta$ divergence b increases monotonically (for $\alpha > 0$) with β . This comes from the fact, that the contribution to the susceptibility Eq.(10) is proportional to the area of the Fermi surface (length of the 1D surface in our case), which decreases with increasing α and shrinks to the Dirac points for $\alpha = \pi/2$ as shown in Fig.(1).

Even though the AF order is expected at $T = 0$, at higher temperature the susceptibility develops minima at $\mathbf{q} \neq \mathbf{q}_\pi$. An example for a diagonal \mathbf{q} , $\mathbf{q} = (q_d, q_d)$, $q_d \in [0, \pi]$ is shown in Fig.(3). Therefore, at this temperature, the linear response analysis predicts an instability towards a different magnetic order. In addition, since these minima correspond to a finite value of the susceptibility χ_m , the phase transition is predicted to occur at a finite interaction $U = -\frac{3}{4} \frac{1}{\chi_m}$. However, this prediction assumes a second order phase transition and at this (large) value of U , another magnetic order might have already appeared. In addition, since the value of the minimum of the susceptibility is not much lower than the one of the AF order, it might explain that, from a numerical point of view (finite size...), the onset of those non-AF phases at finite temperature and finite interaction have not been observed yet.

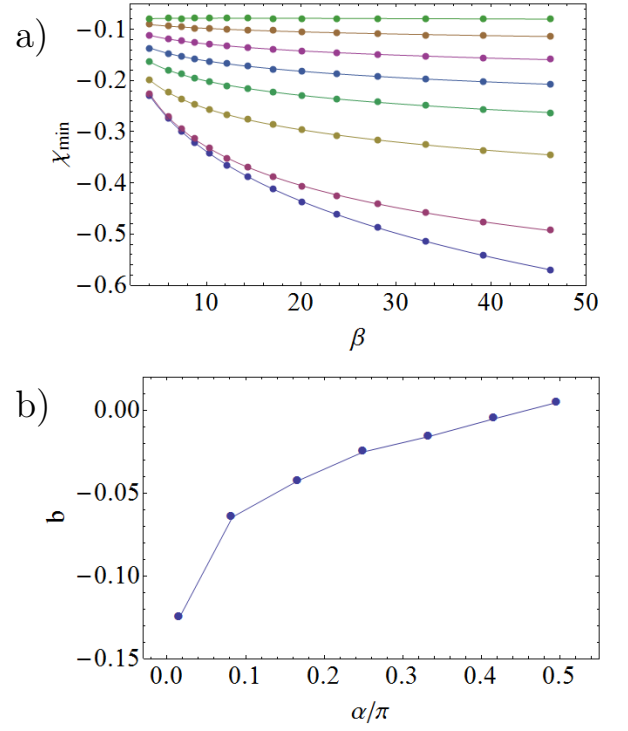


FIG. 2. (Color online) a) Plot of the minimal eigenvalue of χ against β for $\mathbf{q} = (\pi, \pi)$. The data points were calculated using Eq.(10) and the lines are the fits Eq.(16). The lowest curve corresponds to $\alpha = 0$ and the highest to $\alpha = \pi/2$ in monotonically increasing order corresponding to Table I. b) Fitting parameter b against the gauge field parameter $\alpha > 0$ (only non zero values of α). The plot shows a monotonic decrease of $|b|$ - see text for details.

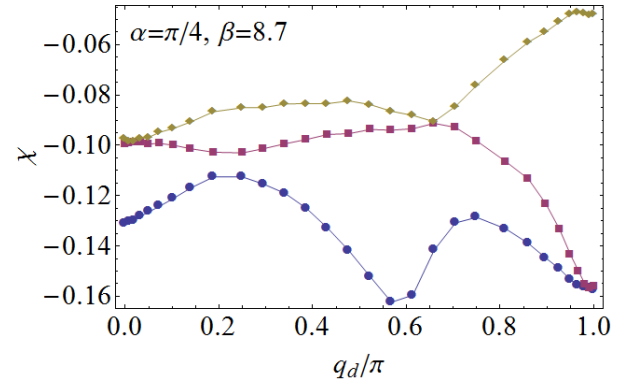


FIG. 3. (Color online) Susceptibility eigenvalues vs. \mathbf{q} on the diagonal of the Brillouin zone, $\mathbf{q} = (q_d, q_d)$. An example for $\alpha = \pi/4$ and $\beta = 8.7$ is shown and demonstrates a minimum of the susceptibility occurring for $\mathbf{q} \neq \mathbf{q}_\pi$.

B. Mean Field numerical simulation

To further investigate the properties of the system, we study the properties of the mean-field Hamiltonian ground state. More precisely, at finite temperature, we minimize the mean-field free energy $F_{\text{MF}} = -\frac{1}{\beta} \ln Z$, where Z is the partition function associated to the mean-field Hamiltonian H_{MF} (See Appendix A for details):

$$H_{\text{MF}} = - \sum_{\mathbf{j}, \mathbf{j}'} c_{\mathbf{j}, s}^\dagger T_{\mathbf{j}, \mathbf{j}'}^{s, s'} c_{\mathbf{j}', s'} - \frac{4U}{3} \sum_{\mathbf{j}} \langle \mathbf{S}_{\mathbf{j}} \rangle \cdot \mathbf{S}_{\mathbf{j}} + \frac{2U}{3} \sum_{\mathbf{j}} \langle \mathbf{S}_{\mathbf{j}} \rangle \cdot \langle \mathbf{S}_{\mathbf{j}} \rangle. \quad (18)$$

At half-filling, with a repulsive interaction, the total average density is expected to remain fixed to unity, the relevant degrees of freedom being the average values of the spin operators S_j^a . The present mean-field decoupling respects thus the $SU(2)$ invariance of the interaction and allows for all possible magnetic orderings, in particular those obtained in the large U limit from the effective Heisenberg model^{20,21}. From that point of view, even though other mean-field decoupling schemes are possible⁴⁰, the present one is expected to capture qualitatively the properties of the magnetic phases for different values of U and α .

The numerical calculation has been performed on a 36×36 square lattice with periodic boundary conditions for different values of parameters α, U, β . On each lattice site, the three components of the spin $\langle \mathbf{S}_{\mathbf{j}} \rangle$ are independent mean-field parameters. Since the mean-field Hamiltonian (18) is quadratic in the fermionic operators, the free energy can be obtained by diagonalizing a $2N \times 2N$ matrix, where N is the number of lattice sites. Even though the exact structure of the matrix is slightly different from the one obtained in the BCS case^{32,41,42}, there is a one to one mapping between the two situations, namely a particle-hole transformation on one of the species. From a numerical point of view, the free energy is minimized using a mixed quasi-Newton and conjugate gradient method; additional checks (e.g. different initial values of the spins) were performed to ensure that the global minimum has been reached. Finally, even though the mean-field calculation captures the temperature dependence of the spin degrees of freedom, it only describes the Mott transition, whereas the determination of the true critical temperature to a quasi-long range magnetic order, especially in the large interaction limit, amounts to taking into account the effects of terms beyond mean field⁴³.

The results are summarized in Table II. Only few values of the gauge field and interaction are presented, since the focus of the paper is on the generic evolution of the system phase from the non-interacting situation to the large interacting limit. For the parameters under consideration, we have identified the following phases: • Antiferromagnet (AF), $\mathbf{q} = (\pi, \pi)$, • Spiral (SI), $\mathbf{q} = (q, q')$,

$\alpha/\pi = 0.1$

10000	AF	SI2
$\beta \backslash U$	2	2.5

$\alpha/\pi = 0.2$

10000		AF+SI	SI
1000	AF		
50		SI	SI
$\beta \backslash U$	3	3.5	4

$\alpha/\pi = 0.25$

1000	AF			
50		SI	SI (coex)	SI (coex)
$\beta \backslash U$	3.5	4	5	6

$\alpha/\pi = 0.3$

50	AF	SI	SI+SkX	SI+SkX	SI+SkX	SkX
$\beta \backslash U$	4.5	4.75	6	6.5	7	10

TABLE II. (Color online) Summary of the MF results. *Legend:* AF (blue) - antiferromagnetic phase, SI (dark red), SI2 (orange) - spiral phases, SkX (yellow) - Skyrminion crystal, see text and Table III for definitions; For fixed values of α , we show phases which occur as a function of β , the inverse temperature, and U , the interaction strength. For small values of the interaction, AF phase occurs for all α and for sufficiently high values of β (low temperatures), in agreement with the results predicted by the linear response theory. For increasing values of U , a phase transition occurs towards different phases (SI, SI2, SkX), depending on α . For other values of α , not shown here, we have found a similar scenario. For $\alpha \geq 0.4\pi$, the logarithmic divergence of the susceptibility with the temperature is very slow, such that the AF phase only appears for very low values of the temperature and, from a numerical point of view, is very difficult to observe with our method. Coexistence of different phases is indicated (either of two well defined phases or of a well defined phase and an unknown phase (coex)).

• Spiral 2 (SI2), $\mathbf{q} = (q, \pi)$, • Skyrminion crystal (SkX), $\mathbf{q} = (\pi, \pm\pi/3)$ and \mathbf{q} is modulo the periodicity of the BZ. As one can see from the Table II, an AF phase always shows up first at low interaction; one can see that when the transition normal-AF occurs for a low interaction, the phase only exists for very low temperature, a behaviour similar to the BCS situation. For other values of α , not shown here, we have found a similar scenario. For $\alpha \geq 0.4\pi$, the logarithmic divergence of the susceptibility with the temperature is very slow, such that the AF phase only appears for very low values of the temperature and, from a numerical point of view, is very difficult to observe with our method.

For larger interaction values, the AF order further evolves to a phase depicting a magnetic texture (spiral...), corresponding to peaks in $|\mathbf{S}(\mathbf{q})|^2$ away from the corner of the BZ. The transition is of first order, since the AF order parameter doesn't vanish at the transition point,

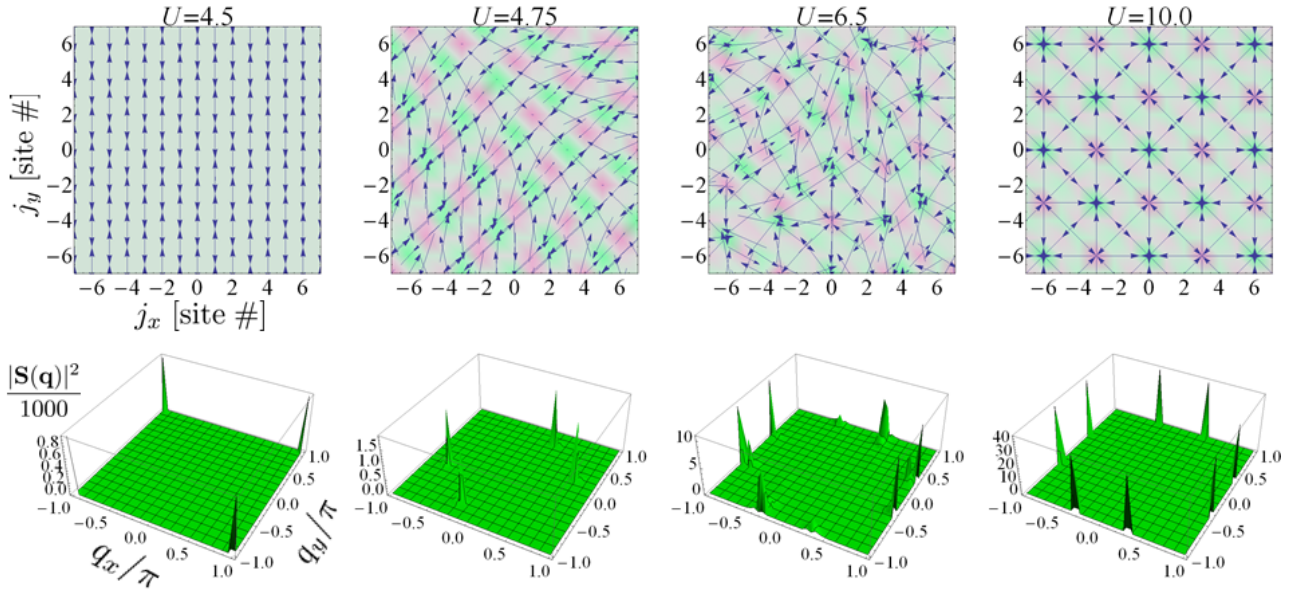


FIG. 4. (Color online) *First row:* Density vector plots of spins $\langle S_j^a \rangle$ for different interaction strengths $U = 4.5, 4.75, 6.5, 10$. We plot the central region of the 36×36 lattice. The real space z component of the spin S_j^z is color encoded, where the pink color corresponds to the maxima and the green color to the minima of S^z respectively. The color scaling is relative to each U independently. *Second row:* 3D plots of the spin density $|S(\mathbf{q})|^2$ in the first Brillouin zone for interaction strengths $U = 4.5, 4.75, 6.5, 10$: $U = 4.5, 4.75, 10$ correspond to AF, SI and SkX phases, which are clearly indicated by peaks of $|S(\mathbf{q})|^2$. $U = 6.5$ corresponds to a crossover between SI and SkX phase, where the two phases coexist. The used parameter values are $\alpha = 0.3\pi$ and $\beta = 50$. See also Table II and Appendix C for quantitative details.

at which also a magnetic texture appears.

Then, for larger interaction strength and depending on the gauge-field parameter, the magnetic texture can further evolve to another phase, to reach finally the spin configuration predicted from the Heisenberg-model. It's more difficult to determine the type of transition from one phase to the other, but from the numerical data it seems to correspond to a smooth change in the location of the peaks of $|S(\mathbf{q})|^2$, i.e. a crossover within the numerical resolution of the simulation.

Finally, one should notice that the critical value $U_c(\alpha)$ of the transition from the AF order is not expected to depict a smooth curve in the $U - \alpha$ plane, since, in the magnetic texture phase, the different mean-field Hamiltonians $H_{\text{MF}}(\alpha)$ have different translational symmetries, a situation similar to the Hofstadter-Hubbard model, depicting fermions (or bosons) in an external magnetic field. Nevertheless, our numerics seems to suggest that the transition from an AF order to a magnetic texture phase increases with the gauge-field parameter α , such that the AF order on the $\alpha = 0$ line seems to be unstable towards a magnetic structure phase in the presence of arbitrary small spin-orbit coupling.

In Fig.(4), an example of a real space spin configuration $\langle S_j^a \rangle$ together with its Fourier transform $|S(\mathbf{q})|^2$ is shown for $\alpha = 0.3\pi$ and $\beta = 50$. Different phases (AF, SI, SkX for $U=4.5, 4.75, 10$) or their coexistence (SI + SkX for $U = 6.5$) are clearly indicated by peaks of $|S(\mathbf{q})|^2$. As one can see, in the large U limit, one recovers

	\mathbf{q}	$\mathbf{N}_1(\mathbf{q}) \times \mathbf{N}_2(\mathbf{q})$	$\mathbf{N}_1(\mathbf{q}) \cdot \mathbf{N}_2(\mathbf{q})$
AF	(π, π)	0	0
SI	(q, q')	$\neq 0$	0
SI2	(q, π)	$\neq 0$	0
SkX	$(\pi, \pm\pi/3)$	non-planar	$\neq 0$

TABLE III. Summary of magnetic phases. Different phases are defined by the value of \mathbf{q} at which $|S(\mathbf{q})|^2$ peaks. Further distinction of magnetic orders given by the values of $\mathbf{N}_1 \cdot \mathbf{N}_2$ and $\mathbf{N}_1 \times \mathbf{N}_2$ is shown. The skyrmion phase (SkX) corresponds to a pair of parameters $(\mathbf{N}_1(\mathbf{q}_{\pm}), \mathbf{N}_2(\mathbf{q}_{\pm}))$ at inequivalent positions \mathbf{q}_{\pm} in the Brillouin zone, with, in addition, non-collinear $\mathbf{N}_1(\mathbf{q}_{\pm}) \times \mathbf{N}_2(\mathbf{q}_{\pm})$ vectors. See also Eq.(19) and the text for details.

the spin configuration expected from the effective Heisenberg model, i.e. a 3×3 Skyrmion crystal which is non-planar magnetic order with a non-vanishing Skyrmion density $\mathbf{S}_j \cdot (\mathbf{S}_{j+1_x} \times \mathbf{S}_{j+1_y})$. The magnetic orders can be parametrized by the peak values of $|S(\mathbf{q})|^2$. More specifically, each peak \mathbf{q} gives rise to a spin wave, which can be described as⁴⁴

$$\langle S_j^a \rangle = N_1^a(\mathbf{q}) \cos \mathbf{q} \cdot \mathbf{j} + N_2^a(\mathbf{q}) \sin \mathbf{q} \cdot \mathbf{j} \quad (19)$$

with further distinction of collinear, $\mathbf{N}_1(\mathbf{q}) \times \mathbf{N}_2(\mathbf{q}) = 0$, and non collinear, $\mathbf{N}_1(\mathbf{q}) \times \mathbf{N}_2(\mathbf{q}) \neq 0$, orders. The values of $\mathbf{q}, \mathbf{N}_1(\mathbf{q})$ and $\mathbf{N}_2(\mathbf{q})$ are summarized in Appendix C.

IV. CONCLUSION

In summary, we have studied the quantum phase transitions of the Fermi-Hubbard model in a square lattice at half-filling in the presence of an effective spin-orbit coupling. We have shown that at small interaction, the system always enters an AF order, then undergoes a first order phase transition to a phase depicting magnetic texture, and, eventually, reaches (at large interaction strength), the magnetic texture predicted by the associated Heisenberg model.

In addition to the half-filling situation presented here, a possible study will concern the doped case or the imbalanced population case, where more exotic mag-

netic phases are expected to occur, possibly in competition with the non-conventional superconductivity. One should also take into account the effects of terms beyond mean field to determine properly the critical temperature of the transition and to estimate the strength of the quantum fluctuations thus allowing for a better comparison with possible experimental results.

Apart from the (magnetic) properties of the ground state, it would be interesting to study the excitations above the ground state, in particular to describe the dynamical response of the system to external perturbations, like the (sudden) quenches of the interaction or the gauge-field, which can efficiently be achieved in cold atomic gases experiments.

-
- ¹ M. Lewenstein et al., Adv. Phys. **56**, 243 (2007).
 - ² I. Bloch, J. Dalibard, and W. Zwerger, Rev. Mod. Phys. **80**, 885 (2008).
 - ³ W. Ketterle, and M. W. Zwierlein, in *Ultra-cold Fermi Gases*, Proceedings of the International School of Physics Enrico Fermi, Varenna, 20-30 June 2006, Course CLXIV, edited by M. Inguscio, W. Ketterle and C. Salomon, IOS Press (Amsterdam), p. 95 (2007).
 - ⁴ Y. J. Lin, R. L. Compton, A. R. Perry, W. D. Phillips, J. V. Porto, and I. B. Spielman, Physical Review Letters **102**, 130401 (2009).
 - ⁵ Y.-J. Lin, R.L. Compton, K. Jiménez-García, J.V. Porto, and I.B. Spielman, Nature (London) **462**, 628 (2009).
 - ⁶ Y.-J. Lin, K. Jiménez-García, and I.B. Spielman, Nature (London) **471**, 83 (2011).
 - ⁷ P. Wang, Z.-Q. Yu, Z. Fu, J. Miao, L. Huang, S. Chai, H. Zhai, and J. Zhang, Phys. Rev. Lett. **109**, 095301 (2012).
 - ⁸ L. W. Cheuk, A. T. Sommer, Z. Hadzibabic, T. Yefsah, W. S. Bakr, and M. W. Zwierlein, Phys. Rev. Lett. **109**, 095302 (2012).
 - ⁹ J. Struck, C. Ölschläger, M. Weinberg, P. Hauke, J. Simonet, A. Eckardt, M. Lewenstein, K. Sengstock, and P. Windpassinger, Phys. Rev. Lett. **108**, 225304 (2012).
 - ¹⁰ K. Jiménez-García, L.J. LeBlanc, R. A. Williams, M. C. Beeler, A. R. Perry, and I. B. Spielman, Phys. Rev. Lett. **108**, 225303 (2012).
 - ¹¹ V. Pietilä and M. Möttönen, Phys. Rev. Lett. **102**, 080403 (2009).
 - ¹² N. Goldman, D.F. Urban, D. Bercioux Phys. Rev. A **83**, 063601 (2011).
 - ¹³ Michele Burrello and Andrea Trombettoni, Phys. Rev. Lett. **105**, 125304 (2010).
 - ¹⁴ Y. Nishida and S. Tan, Phys. Rev. Lett **101**, 170401 (2008).
 - ¹⁵ Y. Nishida, Phys. Rev. A **82**, 011605(R) (2010).
 - ¹⁶ G. Lamporesi et al., Phys. Rev. Lett. **104**, 153202 (2010).
 - ¹⁷ W.-M. Huang, K. Irwin and S.-W. Tsai, Phys. Rev. A **87**, 031603(R) (2013).
 - ¹⁸ M. Iskin and A. L. Subasi, Phys. Rev. A **82**, 063628 (2010).
 - ¹⁹ J. Dalibard, F. Gerbier, G. Juzeliūnas, and P. Öhberg, Rev. Mod. Phys. **83**, 1523 (2011).
 - ²⁰ W. S. Cole, S. Zhang, A. Paramekanti, and N. Trivedi, Phys. Rev. Lett. **109**, 085302 (2012).
 - ²¹ Daniel Cocks, Peter P. Orth, Stephan Rachel, Michael Buchhold, Karyn Le Hur, and Walter Hofstetter, Phys. Rev. Lett. **109**, 205303 (2012) and references therein.
 - ²² N. Goldman, A. Kubasiak, P. Gaspard, and M. Lewenstein, Phys. Rev. A **79**, 023624 (2009).
 - ²³ Z. Cai, X. Zhou, and C. Wu, Phys. Rev. A **85**, 061605(R) (2012).
 - ²⁴ Radić, J. and Di Ciolo, A. and Sun, K. and Galitski, V. Phys. Rev. Lett. **109**, 085303 (2012).
 - ²⁵ M. Sato, Y. Takahashi, and S. Fujimoto, Phys. Rev. Lett. **103**, 020401 (2009).
 - ²⁶ N. Goldman, W. Beugeling, C. Morais-Smith Europhys. Lett. **97**, 23003 (2012).
 - ²⁷ Jayantha P. Vyasankere, Shizhong Zhang, and Vijay B. Shenoy Phys. Rev. B **84**, 014512 (2011)
 - ²⁸ Li Han and C. A. R. Sá de Melo Phys. Rev. A **85**, 011606(R) (2012)
 - ²⁹ A. Kubasiak, P. Massignan, M. Lewenstein, Europhys.Lett. **92**, 46004 (2010).
 - ³⁰ M. Iskin and A.L. Subasi, Phys. Rev. A **84**, 043621 (2011).
 - ³¹ M. Iskin and A.L. Subasi <http://arxiv.org/abs/1211.4020> (2012).
 - ³² M. Iskin, <http://arxiv.org/abs/1304.1473> (2013).
 - ³³ K. Riedl, C. Drukier, P. Zalom, and P. Kopietz Phys. Rev. A **87**, 063626 (2013).
 - ³⁴ A. H. MacDonald, S. M. Girvin, and D. Yoshioka, Phys. Rev. B **37**, 9753 (1988).
 - ³⁵ *Rear Earth Magnetism*, edited by J. Jensen and A. R. Mackintosh (Clarendon Press, Oxford, 1991).
 - ³⁶ *Condensed Matter Field Theory*, edited by A. Altland and B. Simons (Cambridge University Press, ADDRESS, 2010).
 - ³⁷ David Pekker, Mehrtash Babadi, Rajdeep Sensarma, Nikolaj Zinner, Lode Pollet, Martin W. Zwierlein, and Eugene Demler, Phys. Rev. Lett. **106**, 050402 (2011).
 - ³⁸ H. Shimahara and S. Takada, J. Phys. Soc. Jap. **57**, 1044 (1988).
 - ³⁹ In Eq.(16) $C_0 = 0.0166$ and $\gamma \approx 0.5772$ is the Euler gamma. For the tunneling amplitude $t = 1$, we have to set the tunneling amplitude $\tilde{t} = 2$ in³⁸ due to the factor 2 of difference in the definition of eigenenergies. In addition, for $\alpha = 0$, the unitary matrices in the definition of \mathcal{S}

Eq.(12) reduce to the identities and we are left with

$$\sum_{\mathbf{k}, s, s'} (S_{\mathbf{k}, \mathbf{k}+\mathbf{q}}^a)_{s, s'} (S_{\mathbf{k}+\mathbf{q}, \mathbf{k}}^b)_{s', s} F(\mathbf{k}) = \sum_{\mathbf{k}} F(\mathbf{k}) \frac{1}{4} \sum_{s, s'} \sigma_{ss'}^a \sigma_{s's}^b$$

In this case, the last sum over elements of the Pauli matrices is 0 for $a \neq b$ and 2 for $a = b$ as can be easily verified. This gives purely diagonal susceptibility, as expected for $\alpha = 0$. It also yields an additional factor of 2 between the definition Eq.(10) and the formula Eq.(17).

⁴⁰ H.J. Schultz, Phys. Rev. Lett. **65**, 2462 (1990).

⁴¹ Y. Dubi and Y. Avishai, Nature **449**, 876 (2007).

⁴² Y. Chen, Z.D. Wang, F.C. Zhang, C.S. Ting, Phys. Rev. B **79**, 054512 (2009).

⁴³ J.R. Engelbrecht, M. Randeria, and C.A.R. Sá de Melo, Phys. Rev. B **55**, 15153 (1997).

⁴⁴ S. Sachdev, Rev. Mod. Phys. **75**, 913 (2003).

⁴⁵ *Atom-Photon Interactions*, edited by C. C. Tannoudji, J. Dupont-Roc, and G. Grynberg (John Wiley & Sons, New York, 1998).

Appendix A: Linear response of the spin systems

From the linear response theory^{35,36}, the expression for the spin-spin susceptibility $\chi_{\mathbf{q}}^{a,b}(\tau)$ reads:

$$\chi_{\mathbf{q}}^{a,b}(\tau) = -i\theta(\tau) \langle [S_{\mathbf{q}}^a(\tau), S_{-\mathbf{q}}^b(0)] \rangle. \quad (\text{A1})$$

The frequency domain susceptibility is given by the Fourier transform $\chi_{\mathbf{q}}^{a,b}(\omega) = \int d\tau e^{-i\omega\tau} \chi_{\mathbf{q}}^{a,b}(\tau)$.

We can now find an explicit analytical expression for $\chi_{\mathbf{q}}^{a,b}(\omega)$, given the Hamiltonian Eq.(2a - 2c). Namely we need to evaluate the thermal average

$$\langle [S_{\mathbf{q}}^a(\tau), S_{-\mathbf{q}}^b(0)] \rangle = Z^{-1} \text{Tr} \left[(S_{\mathbf{q}}^a(\tau) S_{-\mathbf{q}}^b(0) - S_{-\mathbf{q}}^b(0) S_{\mathbf{q}}^a(\tau)) e^{-\beta H_0} \right]. \quad (\text{A2})$$

In order to evaluate the trace and the time dependence, one needs to diagonalize H_0 . As explained in the main text, this is achieved by going to momentum space and finding 2×2 unitary transform $U_{\mathbf{k}}$ ($d_{\mathbf{k}} = U_{\mathbf{k}} c_{\mathbf{k}}$) such that

$$H_0 = \sum_{\mathbf{k}, s} \epsilon_{\mathbf{k}, s} d_{\mathbf{k}, s}^\dagger d_{\mathbf{k}, s}. \quad (\text{A3})$$

In the diagonal basis, the time evolution of the operators $d_{\mathbf{k}, s}$ is simple, such that one obtains readily the time evolution of the spin operators:

$$S_{\mathbf{q}}^a(\tau) = \sum_{\mathbf{k}} d_{\mathbf{k}, s}^\dagger (S_{\mathbf{k}, \mathbf{k}+\mathbf{q}}^a)_{s, s'} d_{\mathbf{k}+\mathbf{q}, s'} e^{i\tau(\epsilon_{\mathbf{k}, s} - \epsilon_{\mathbf{k}+\mathbf{q}, s'})}, \quad (\text{A4})$$

where

$$S_{\mathbf{k}, \mathbf{k}+\mathbf{q}}^a = \frac{1}{2} U_{\mathbf{k}} \sigma^a U_{\mathbf{k}+\mathbf{q}}^\dagger. \quad (\text{A5})$$

We proceed with the evaluation of the trace Eq.(A2). Lets start with the first part of the commutator

$$\begin{aligned} \text{Tr} (S_{\mathbf{q}}^a(\tau) S_{-\mathbf{q}}^b(0) e^{-\beta H_0}) &= \sum_{n_i} \langle n_1 | S_{\mathbf{q}}^a(\tau) | n_2 \rangle \langle n_2 | S_{-\mathbf{q}}^b(0) | n_3 \rangle \langle n_3 | e^{-\beta H_0} | n_1 \rangle \\ &= \sum S_{\mathbf{q}}^a(\tau)_{n_1, n_2} S_{-\mathbf{q}}^b(0)_{n_2, n_1} [e^{-\beta H_0}]_{n_1, n_1}, \end{aligned} \quad (\text{A6})$$

where the sum runs over complete basis (i.e. momentum and spin) $|n_i\rangle$ and we have used the fact, that H_0 is already diagonalized. Plugging the expression Eq.(A4) to Eq.(A6) one finds

$$\begin{aligned} \text{Tr} (S_{\mathbf{q}}^a(\tau) S_{-\mathbf{q}}^b(0) e^{-\beta H_0}) &= \\ &= \text{Tr} \left(d_{\mathbf{k}, s}^\dagger (S_{\mathbf{k}, \mathbf{k}+\mathbf{q}}^a)_{s, \sigma} d_{\mathbf{k}+\mathbf{q}, \sigma} d_{\mathbf{k}', s'}^\dagger (S_{\mathbf{k}', \mathbf{k}'-\mathbf{q}}^b)_{s', \sigma'} d_{\mathbf{k}'-\mathbf{q}, \sigma'} e^{-i\tau(\epsilon_{\mathbf{k}', s'} - \epsilon_{\mathbf{k}'-\mathbf{q}, \sigma'})} e^{-\beta \sum \epsilon_{\mathbf{p}, \sigma} d_{\mathbf{p}, \sigma}^\dagger d_{\mathbf{p}, \sigma}} \right) \\ &= \text{Tr} \left(d_{\mathbf{k}, s}^\dagger (S_{\mathbf{k}, \mathbf{k}+\mathbf{q}}^a)_{s, s'} d_{\mathbf{k}+\mathbf{q}, s'} d_{\mathbf{k}+\mathbf{q}, s'}^\dagger (S_{\mathbf{k}+\mathbf{q}, \mathbf{k}}^b)_{s', s} d_{\mathbf{k}, s} e^{-i\tau(\epsilon_{\mathbf{k}+\mathbf{q}, s'} - \epsilon_{\mathbf{k}, s})} e^{-\beta \sum \epsilon_{\mathbf{p}, \sigma} d_{\mathbf{p}, \sigma}^\dagger d_{\mathbf{p}, \sigma}} \right). \end{aligned} \quad (\text{A7})$$

Following Eq.(A6), we put in the previous $\mathbf{k}' = \mathbf{k} + \mathbf{q}$ and $\sigma = s'$, $\sigma' = s$. One obtains

$$\begin{aligned}
\text{Tr} \quad & (S_{\mathbf{q}}^a(\tau) S_{-\mathbf{q}}^b(0) e^{-\beta H_0}) = \\
& = Z \sum_{\mathbf{k}, s, s'} (\mathcal{S}_{\mathbf{k}, \mathbf{k}+\mathbf{q}}^a)_{s, s'} (\mathcal{S}_{\mathbf{k}+\mathbf{q}, \mathbf{k}}^b)_{s', s} e^{-i\tau(\epsilon_{\mathbf{k}+\mathbf{q}, s'} - \epsilon_{\mathbf{k}, s})} \frac{e^{-\beta \epsilon_{\mathbf{k}, s}}}{(1 + e^{-\beta \epsilon_{\mathbf{k}, s}})(1 + e^{-\beta \epsilon_{\mathbf{k}+\mathbf{q}, s'}})}, \quad \mathbf{q} \neq 0 \\
& = Z \left\{ \sum_{\mathbf{k}, s \neq s'} (\mathcal{S}_{\mathbf{k}, \mathbf{k}}^a)_{s, s'} (\mathcal{S}_{\mathbf{k}, \mathbf{k}}^b)_{s', s} e^{-i\tau(\epsilon_{\mathbf{k}, s'} - \epsilon_{\mathbf{k}, s})} \frac{e^{-\beta \epsilon_{\mathbf{k}, s}}}{(1 + e^{-\beta \epsilon_{\mathbf{k}, s}})(1 + e^{-\beta \epsilon_{\mathbf{k}, s'}})} \right. \\
& \quad \left. + \sum_{\mathbf{k}, s} (\mathcal{S}_{\mathbf{k}, \mathbf{k}}^a)_{s, s} (\mathcal{S}_{\mathbf{k}, \mathbf{k}}^b)_{s, s} e^{-i\tau(\epsilon_{\mathbf{k}, s'} - \epsilon_{\mathbf{k}, s})} \frac{e^{-\beta \epsilon_{\mathbf{k}, s}}}{1 + e^{-\beta \epsilon_{\mathbf{k}, s}}} \right\}, \quad \mathbf{q} = 0.
\end{aligned} \tag{A8}$$

The trace of $S_{-\mathbf{q}}^b(0) S_{\mathbf{q}}^a(\tau) e^{-\beta H_0}$ is obtained in a similar way and yields a result identical to Eq.(A8) with exchange $\beta \epsilon_{\mathbf{k}, s} \leftrightarrow \beta \epsilon_{\mathbf{k}+\mathbf{q}, s'}$ (i.e. the energies are exchanged only in the thermal terms including β). We next notice, that

$$\begin{aligned}
\frac{e^{-\beta \epsilon_a} - e^{-\beta \epsilon_b}}{(1 + e^{-\beta \epsilon_a})(1 + e^{-\beta \epsilon_b})} &= \frac{e^{-\beta \epsilon_a} + 1 - 1 - e^{-\beta \epsilon_b}}{(1 + e^{-\beta \epsilon_a})(1 + e^{-\beta \epsilon_b})} \\
&= \frac{1}{1 + e^{-\beta \epsilon_b}} - \frac{1}{1 + e^{-\beta \epsilon_a}} = (1 - n(\epsilon_b)) - (1 - n(\epsilon_a)) \\
&= n(\epsilon_a) - n(\epsilon_b).
\end{aligned} \tag{A9}$$

This also holds for the degenerate case ($\mathbf{q} = \mathbf{0}$, last line in Eq.(A8)), in which we have directly

$$\frac{e^{-\beta \epsilon_a}}{1 + e^{-\beta \epsilon_a}} - \frac{e^{-\beta \epsilon_b}}{1 + e^{-\beta \epsilon_b}} = n(\epsilon_a) - n(\epsilon_b). \tag{A10}$$

We obtain the result for the trace of the commutator

$$\langle [S_{\mathbf{q}}^a(\tau), S_{-\mathbf{q}}^b(0)] \rangle = \sum_{\mathbf{k}, s, s'} (\mathcal{S}_{\mathbf{k}, \mathbf{k}+\mathbf{q}}^a)_{s, s'} (\mathcal{S}_{\mathbf{k}+\mathbf{q}, \mathbf{k}}^b)_{s', s} (n(\epsilon_{\mathbf{k}, s}) - n(\epsilon_{\mathbf{k}+\mathbf{q}, s'})) e^{-i\tau(\epsilon_{\mathbf{k}+\mathbf{q}, s'} - \epsilon_{\mathbf{k}, s})}. \tag{A11}$$

The only time dependent factor is the oscillating exponential and we can thus directly compute the time integral in the definition of the susceptibility Eq.(A1)

$$\begin{aligned}
-i \int_{-\infty}^{\infty} d\tau e^{i\omega\tau} \theta(\tau) e^{-i\tau(\epsilon_{\mathbf{k}+\mathbf{q}, s'} - \epsilon_{\mathbf{k}, s})} &= -i \int_0^{\infty} dt e^{i\omega\tau - \eta\tau} e^{-i\tau(\epsilon_{\mathbf{k}+\mathbf{q}, s'} - \epsilon_{\mathbf{k}, s})} \\
&= \frac{1}{\omega + \epsilon_{\mathbf{k}, s'} - \epsilon_{\mathbf{k}+\mathbf{q}, s} + i\eta},
\end{aligned} \tag{A12}$$

where we have added the infinitesimal convergence factor η . Plugging this back to the defining relation for the susceptibility Eq.(A1), we obtain the final result for the susceptibility of the non interacting system

$$\chi_{\mathbf{q}}^{a,b}(\omega) = \frac{1}{N} \sum_{\mathbf{k}, s, s'} (\mathcal{S}_{\mathbf{k}, \mathbf{k}+\mathbf{q}}^a)_{s, s'} (\mathcal{S}_{\mathbf{k}+\mathbf{q}, \mathbf{k}}^b)_{s', s} \frac{n(\epsilon_{\mathbf{k}, s'}) - n(\epsilon_{\mathbf{k}+\mathbf{q}, s})}{\omega + \epsilon_{\mathbf{k}, s'} - \epsilon_{\mathbf{k}+\mathbf{q}, s} + i\eta}. \tag{A13}$$

Susceptibility in the interacting MF model

We have derived the susceptibility Eq.(A13) for the non-interacting system subjected to a small external driving force. We will now use this result to find a susceptibility of the interacting system described by the mean-field theory. Lets recall the interaction Hamiltonian Eq.(3):

$$\begin{aligned}
H_{\text{int}} &= -\frac{2U}{3} \sum_{\mathbf{j}} S_{\mathbf{j}}^b(t) S_{\mathbf{j}}^b(t) = -\frac{2U}{3} \frac{1}{N} \sum_{\mathbf{q}} S_{-\mathbf{q}}^b(t) S_{\mathbf{q}}^b(t) \\
&\stackrel{\text{MF}}{=} \frac{-g}{N} \sum_{\mathbf{q}} \langle S_{-\mathbf{q}} \rangle \langle S_{\mathbf{q}} \rangle + \langle S_{-\mathbf{q}} \rangle (S_{\mathbf{q}} - \langle S_{\mathbf{q}} \rangle) + (S_{-\mathbf{q}} - \langle S_{-\mathbf{q}} \rangle) \langle S_{\mathbf{q}} \rangle + O((\delta S)^2) \\
&= \frac{-g}{N} \sum_{\mathbf{q}} 2S_{-\mathbf{q}} \langle S_{\mathbf{q}} \rangle - \langle S_{-\mathbf{q}} \rangle \langle S_{\mathbf{q}} \rangle = H_{\text{int}}^{\text{MF}},
\end{aligned} \tag{A14}$$

where we have introduced the coupling strength $g = 2U/3$. In the last line of the preceding equation, the last term does not contribute to the spin dynamics and is normalized out in the computation of the spin average values. We thus drop this term. We obtain the effective external driving Hamiltonian

$$H_{\text{ext}}^{\text{eff}} = H_{\text{ext}} + H_{\text{int}}^{\text{MF}} = \frac{1}{N} \sum_{\mathbf{q}} S_{-\mathbf{q}}^b(t) [B_{\mathbf{q}}^b(t) - 2g\langle S_{\mathbf{q}}^b \rangle(t)] = \frac{1}{N} \sum_{\mathbf{q}} S_{-\mathbf{q}}^b(t) (B_{\mathbf{q}}^b)^{\text{eff}}(t). \quad (\text{A15})$$

We can thus see, that the inclusion of the MF interaction amounts to replacing the external driving B by the new effective driving B^{eff} . One then follows the same procedure as in the non interacting case. Since we are mainly interested in the frequency response of the system, we will use the defining formula connecting the frequency components of the spins with the driving through the susceptibility

$$\langle S_{\mathbf{q}}^a(\omega) \rangle = \chi_{\mathbf{q}}^{a,b}(\omega) (B_{\mathbf{q}}^b)^{\text{eff}}(\omega). \quad (\text{A16})$$

One can easily check, that the frequency components of the effective driving are given by the Fourier transform of its parts,

$$\begin{aligned} (B_{\mathbf{q}}^b)^{\text{eff}}(\omega) &= \int dt e^{i\omega t} (B_{\mathbf{q}}^b(t) - 2g\bar{S}_{\mathbf{q}}^b(t)) \\ &= B_{\mathbf{q}}^b(\omega) - 2g\bar{S}_{\mathbf{q}}^b(\omega). \end{aligned} \quad (\text{A17})$$

Therefore, one obtains

$$\langle S_{\mathbf{q}}^a \rangle(\omega) = \sum_b \chi_{\mathbf{q}}^{a,b}(\omega) B_{\mathbf{q}}^b(\omega) - 2g\langle S_{\mathbf{q}}^b \rangle(\omega), \quad (\text{A18})$$

which after a straightforward manipulation yields the equation for the average value of the spin operators

$$\begin{aligned} \langle \mathbf{S}_{\mathbf{q}} \rangle(\omega) &= M^{-1} \chi \mathbf{B} \\ M^{a,b} &= \delta^{a,b} + 2g\chi_{\mathbf{q}}^{a,b}(\omega), \end{aligned} \quad (\text{A19})$$

where we merely rewrote the equation Eq.(A18) in the symbolic matrix notation. From here, one can obtain the information about the critical value of the coupling strength g (and thus U) from the divergences of the average of the spin operators, i.e. when the matrix M becomes singular.

Appendix B: Effective Heisenberg model in the large U limit

We now restrict our interest to the regime with strong repulsion, high U . In this regime, the ground state of the grand canonical ensemble has single occupation at each site. Moreover it would cost an energy of order of U to increase the double occupancy by one. This regime can be described by the method of effective Hamiltonian, which is suitable for systems with well separated energy manifolds⁴⁵. The energy manifolds are separated by U and we would like to evaluate the effect of the coupling between the ground state manifold and the higher lying manifolds. This coupling results in the perturbation of the bare energy levels in the ground state manifold. In this section, we present the treatment used in³⁴ and⁴⁵ (page 38).

In the following we consider a situation at half filling $\mu_1 = \mu_2 = 0$. When we multiply the kinetic Hamiltonian Eq.(2a) by $n_{\mathbf{j},\bar{s}} + h_{\mathbf{j},\bar{s}} = 1$ from the left and by $n_{\mathbf{j}',\bar{s}'} + h_{\mathbf{j}',\bar{s}'} = 1$ from the right, we obtain

$$H_{\text{kin}} \equiv T = T_0 + T_{-1} + T_1, \quad (\text{B1})$$

where

$$\begin{aligned} T_0 &= - \sum n_{\mathbf{j},\bar{s}} c_{\mathbf{j},s}^\dagger T_{\mathbf{j},\mathbf{j}'}^{s,s'} c_{\mathbf{j}',s'} n_{\mathbf{j}',\bar{s}'} + h_{\mathbf{j},\bar{s}} c_{\mathbf{j},s}^\dagger T_{\mathbf{j},\mathbf{j}'}^{s,s'} c_{\mathbf{j}',s'} h_{\mathbf{j}',\bar{s}'} \\ T_{-1} &= - \sum h_{\mathbf{j},\bar{s}} c_{\mathbf{j},s}^\dagger T_{\mathbf{j},\mathbf{j}'}^{s,s'} c_{\mathbf{j}',s'} n_{\mathbf{j}',\bar{s}'} \\ T_1 &= - \sum n_{\mathbf{j},\bar{s}} c_{\mathbf{j},s}^\dagger T_{\mathbf{j},\mathbf{j}'}^{s,s'} c_{\mathbf{j}',s'} h_{\mathbf{j}',\bar{s}'}, \end{aligned} \quad (\text{B2})$$

where n and h denote the particle and hole number operators respectively and \bar{s}, \bar{s}' denote the spin orthogonal to s, s' - e.g. \bar{s} is spin up for s spin down and vice versa. The sums in Eq.(B2) run over nearest neighbours $\langle \mathbf{j}, \mathbf{j}' \rangle$ and spins

s, s' . Denoting the interaction Hamiltonian Eq.(2c) as V , one can easily verify the following commutation relations

$$\begin{aligned} [V, T_0] &= 0 \\ [V, T_{-1}] &= -UT_{-1} \\ [V, T_1] &= UT_1, \end{aligned} \quad (\text{B3})$$

which can be summarized as

$$[V, T_m] = mUT_m. \quad (\text{B4})$$

We are now ready to proceed with the effective Hamiltonian derivation. We wish to rewrite the current Hamiltonian $H = V + T$ as

$$H_{\text{eff}} = e^{iS} H e^{-iS} = H + [iS, H] + \frac{1}{2!} [iS, [iS, H]] + \dots = \sum_{n=0}^{\infty} \frac{1}{n!} [iS, H]^{(n)}, \quad (\text{B5})$$

where S is some Hermitian matrix (we require the transformation to be unitary). $[iS, H]^{(n)}$ denotes the n -times nested commutator and $[iS, H]^{(0)} = H$. The matrix S can be determined in the following way. Lets write S as

$$S = \lambda S_1 + \lambda^2 S_2 + \dots = \sum_{n=1}^{\infty} \lambda^n S_n, \quad (\text{B6})$$

where $\lambda = 1/U$ is our small parameter around which we will do our perturbative expansion. The elements of the matrix S_k can be determined in an iterative way by requiring, that after the unitary transformation up to the order k in the expansion Eq.(B5) all terms bringing the energy out of the ground state manifold have to vanish. We also denote

$$S^{(k)} = \sum_{n=1}^k \lambda^n S_n \quad (\text{B7})$$

Important thing to note is that the energy ratio between V and T is of order λ^{-1} . It is thus more transparent to rewrite the Hamiltonian as $H = V + \lambda \tilde{T}$, where V and $\tilde{T} = \lambda^{-1}T$ are now contributions of the same order. With this notation, the commutator Eq.(B4) can be written as

$$\lambda [V, \tilde{T}_m] = m\tilde{T}_m. \quad (\text{B8})$$

In the first order in λ we have from Eq.(B5)

$$H_{\text{eff}} = H + [i\lambda S_1, H] = V + \lambda(\tilde{T}_0 + \tilde{T}_{-1} + \tilde{T}_1) + \lambda[iS_1, V] + \dots \quad (\text{B9})$$

The terms which bring one from the ground state manifold are the terms changing the double occupancy, i.e. \tilde{T}_{-1} and \tilde{T}_1 . In order to cancel these terms with the commutator, one gets

$$iS_1 = \lambda(\tilde{T}_1 - \tilde{T}_{-1}). \quad (\text{B10})$$

We will now generalize this procedure in an iterative way to arbitrarily high order in λ . Lets define a Hamiltonian of order $k+1$ as

$$H^{(k+1)} = e^{iS^{(k)}} H e^{-iS^{(k)}} = \sum_{n=0}^{\infty} \frac{1}{n!} [iS^{(k)}, H]^{(n)}. \quad (\text{B11})$$

As a matter of example, lets take $k=1$

$$\begin{aligned} H^{(2)} &= H + \lambda[iS_1, H] + \frac{\lambda^2}{2} \lambda[iS_1, [iS_1, H]] + O(\lambda^3) \\ &= H + \lambda[iS_1, V] + \lambda^2[iS_1, \tilde{T}] + \frac{\lambda^2}{2} [iS_1, [iS_1, V]] + O(\lambda^3). \end{aligned} \quad (\text{B12})$$

The last two terms in the second line are of the same order λ since $S_1 \propto 1$ and $V \propto \lambda^{-1}$. The idea is now to use this Hamiltonian to find the explicit form of the next elements in the expansion of iS , namely the element iS_2 . This can be done as follows. The third order Hamiltonian can be written as

$$H^{(3)} = H_0^{(2)} + H_{\text{ch}}^{(2)} + \lambda^2 [iS_2, V] + O(\lambda^3), \quad (\text{B13})$$

where we have decomposed the second order Hamiltonian into a part which does not change the double occupancy $H_0^{(2)}$ and the one which changes the double occupancy, $H_{\text{ch}}^{(2)}$. We require, that the lowest order term of iS_2 cancels the double occupancy changing term. This is the general procedure for an arbitrary order expansion, so that

$$H^{(k+1)} = H_0^{(k)} + H_{\text{ch}}^{(k)} + \lambda^k [iS_k, V] + O(\lambda^{k+1}). \quad (\text{B14})$$

In order to find the explicit form of iS_k , we will need the following relationships. Lets denote the product of tunnelling operators as

$$\tilde{T}^k(m) \equiv \tilde{T}_{m_1} \dots \tilde{T}_{m_k}. \quad (\text{B15})$$

The commutator with V then reads

$$\lambda [V, \tilde{T}^k(m)] = M^k(m) \tilde{T}^k(m), \quad (\text{B16})$$

where $M^k(m) = \sum_i m_i$. Looking at Eq.(B14), one can write the last two terms as

$$H_{\text{ch}}^{(k)} + \lambda^k [iS_k, V] = \lambda^{2k-1} \sum_m C^k(m) \tilde{T}^k(m) + \lambda^k [iS_k, V] = 0. \quad (\text{B17})$$

The last equality can be achieved by noting that

$$\lambda [V, \tilde{T}^k(m)] \cdot \lambda^{2k-1} \frac{C^k(m)}{M^k(m)} = \lambda^{2k-1} C^k(m) \tilde{T}^k(m), \quad (\text{B18})$$

so that we finally obtain

$$iS_k = \lambda^k \sum_m \frac{C^k(m)}{M^k(m)} \tilde{T}^k(m). \quad (\text{B19})$$

Note that since $M^k(m) \neq 0$ for double occupancy changing T^k , we can safely divide by it.

We have implemented the above described iterative procedure in Mathematica for general tunnellings $T_{\mathbf{j},\mathbf{j}'}^{s,s'}$. Up to the second order in the $1/U$ expansion, one obtains the following effective Heisenberg Hamiltonian ($\delta = x, y$ are the spatial directions in the 2D lattice)

$$H = H_c + \sum_{\delta=x,y} \sum_{<i,i+\delta>} \sum_{a=x,y,z} J_{\delta}^a S_i^a S_{i+\delta}^a + \mathbf{D}_{\delta+} \cdot (\mathbf{S}_i \times \mathbf{S}_{i+\delta})_+ + \mathbf{D}_{\delta-} \cdot (\mathbf{S}_i \times \mathbf{S}_{i+\delta})_-,$$

where

$$\begin{aligned} (\mathbf{S}_i \times \mathbf{S}_{i+\delta})_+ &= (S_1^y S_2^z, S_1^z S_2^x, S_1^x S_2^y) \\ (\mathbf{S}_i \times \mathbf{S}_{i+\delta})_- &= -(S_1^z S_2^y, S_1^x S_2^z, S_1^y S_2^x) \end{aligned}$$

are the "positive" and "negative" part of the vector product. In the most general case, the coefficients read:

$$\begin{aligned} J_{\delta}^x &= 2\lambda \left(T_{\delta}^{2,2} T_{\delta}^{1,1*} + T_{\delta}^{1,2} T_{\delta}^{2,1*} + T_{\delta}^{2,1} T_{\delta}^{1,2*} + T_{\delta}^{1,1} T_{\delta}^{2,2*} \right) \\ J_{\delta}^y &= 2\lambda \left(T_{\delta}^{2,2} T_{\delta}^{1,1*} - T_{\delta}^{1,2} T_{\delta}^{2,1*} - T_{\delta}^{2,1} T_{\delta}^{1,2*} + T_{\delta}^{1,1} T_{\delta}^{2,2*} \right) \\ J_{\delta}^z &= 2\lambda \left(T_{\delta}^{1,1} T_{\delta}^{1,1*} - T_{\delta}^{2,1} T_{\delta}^{2,1*} - T_{\delta}^{1,2} T_{\delta}^{1,2*} + T_{\delta}^{2,2} T_{\delta}^{2,2*} \right) \\ D_{\delta+}^1 &= 2i\lambda \left(-T_{\delta}^{2,1} T_{\delta}^{1,1*} + T_{\delta}^{1,1} T_{\delta}^{2,1*} + T_{\delta}^{2,2} T_{\delta}^{1,2*} - T_{\delta}^{1,2} T_{\delta}^{2,2*} \right) \\ D_{\delta+}^2 &= 2\lambda \left(T_{\delta}^{1,2} T_{\delta}^{1,1*} - T_{\delta}^{2,2} T_{\delta}^{2,1*} + T_{\delta}^{1,1} T_{\delta}^{1,2*} - T_{\delta}^{2,1} T_{\delta}^{2,2*} \right) \\ D_{\delta+}^3 &= 2i\lambda \left(T_{\delta}^{2,2} T_{\delta}^{1,1*} + T_{\delta}^{1,2} T_{\delta}^{2,1*} - T_{\delta}^{2,1} T_{\delta}^{1,2*} - T_{\delta}^{1,1} T_{\delta}^{2,2*} \right) \end{aligned}$$

$$\begin{aligned}
D_{\delta-}^1 &= 2i\lambda \left(-T_{\delta}^{1,2}T_{\delta}^{1,1*} + T_{\delta}^{2,2}T_{\delta}^{2,1*} + T_{\delta}^{1,1}T_{\delta}^{1,2*} - T_{\delta}^{2,1}T_{\delta}^{2,2*} \right) \\
D_{\delta-}^2 &= 2\lambda \left(-T_{\delta}^{2,1}T_{\delta}^{1,1*} - T_{\delta}^{1,1}T_{\delta}^{2,1*} + T_{\delta}^{2,2}T_{\delta}^{1,2*} + T_{\delta}^{1,2}T_{\delta}^{2,2*} \right) \\
D_{\delta-}^3 &= 2i\lambda \left(T_{\delta}^{2,2}T_{\delta}^{1,1*} - T_{\delta}^{1,2}T_{\delta}^{2,1*} + T_{\delta}^{2,1}T_{\delta}^{1,2*} - T_{\delta}^{1,1}T_{\delta}^{2,2*} \right) \\
H_c &= 2\lambda \left(-T_{\delta}^{1,1}T_{\delta}^{1,1*} - T_{\delta}^{2,1}T_{\delta}^{2,1*} - T_{\delta}^{1,2}T_{\delta}^{1,2*} - T_{\delta}^{2,2}T_{\delta}^{2,2*} \right) \frac{1}{4}
\end{aligned}$$

Appendix C: Magnetic orders

In Table IV we list the details of the magnetic orders parametrized by Eq.(19) and summarized in Table III. The tables have the following format

$\{\alpha, U, \beta\}, \text{Phase}$							
q_x/π	q_y/π	N_1^x	N_2^x	N_1^y	N_2^y	N_1^z	N_2^z

$\{\alpha, U, \beta\} = \{0.1, 2.0, 10000\}$, AF

q_x/π	q_y/π	N_1^x	N_2^x	N_1^y	N_2^y	N_1^z	N_2^z
-1	1	1.8×10^{-2}	0	-1.8×10^{-2}	0	0	0
1	1	1.8×10^{-2}	0	-1.8×10^{-2}	0	0	0

$\{\alpha, U, \beta\} = \{0.1, 2.5, 10000\}$, SI2

q_x/π	q_y/π	N_1^x	N_2^x	N_1^y	N_2^y	N_1^z	N_2^z
-1	$\frac{13}{18}$	0	0	-5.3×10^{-2}	8.5×10^{-2}	-9.4×10^{-2}	-5.8×10^{-2}
1	$\frac{13}{18}$	0	0	-5.3×10^{-2}	8.5×10^{-2}	-9.4×10^{-2}	-5.8×10^{-2}

$\{\alpha, U, \beta\} = \{0.2, 3.0, 1000\}$, AF

q_x/π	q_y/π	N_1^x	N_2^x	N_1^y	N_2^y	N_1^z	N_2^z
-1	1	2.1×10^{-2}	0	-2.1×10^{-2}	0	0	0
1	1	2.1×10^{-2}	0	-2.1×10^{-2}	0	0	0

$\{\alpha, U, \beta\} = \{0.2, 3.5, 50\}$, SI

q_x/π	q_y/π	N_1^x	N_2^x	N_1^y	N_2^y	N_1^z	N_2^z
$-\frac{5}{6}$	$\frac{5}{9}$	-4.4×10^{-3}	-2.1×10^{-2}	9.3×10^{-3}	4.5×10^{-2}	-4.2×10^{-2}	8.8×10^{-3}
$\frac{5}{6}$	$\frac{5}{9}$	-2.2×10^{-2}	4.5×10^{-4}	-4.6×10^{-2}	9.4×10^{-4}	-8.9×10^{-4}	-4.3×10^{-2}

$\{\alpha, U, \beta\} = \{0.2, 4.0, 10000\}$, SI

q_x/π	q_y/π	N_1^x	N_2^x	N_1^y	N_2^y	N_1^z	N_2^z
$-\frac{1}{2}$	$\frac{8}{9}$	1.1×10^{-1}	2.9×10^{-2}	-3.8×10^{-2}	$-1. \times 10^{-2}$	2.7×10^{-2}	$-1. \times 10^{-1}$
$\frac{1}{2}$	$\frac{8}{9}$	2.9×10^{-2}	-1.1×10^{-1}	$1. \times 10^{-2}$	-3.8×10^{-2}	$1. \times 10^{-1}$	2.7×10^{-2}

$\{\alpha, U, \beta\} = \{0.2, 4.0, 50\}$, SI

q_x/π	q_y/π	N_1^x	N_2^x	N_1^y	N_2^y	N_1^z	N_2^z
$-\frac{1}{2}$	$\frac{8}{9}$	1.1×10^{-1}	2.9×10^{-2}	-3.8×10^{-2}	$-1. \times 10^{-2}$	2.7×10^{-2}	$-1. \times 10^{-1}$
$\frac{1}{2}$	$\frac{8}{9}$	2.9×10^{-2}	-1.1×10^{-1}	$1. \times 10^{-2}$	-3.8×10^{-2}	$1. \times 10^{-1}$	2.7×10^{-2}

$\{\alpha, U, \beta\} = \{0.25, 3.5, 1000\}$, AF

q_x/π	q_y/π	N_1^x	N_2^x	N_1^y	N_2^y	N_1^z	N_2^z
-1	1	1.6×10^{-2}	0	-4.4×10^{-2}	0	0	0
1	1	1.6×10^{-2}	0	-4.4×10^{-2}	0	0	0

$\{\alpha, U, \beta\} = \{0.25, 4.0, 50\}$, SI

q_x/π	q_y/π	N_1^x	N_2^x	N_1^y	N_2^y	N_1^z	N_2^z
$-\frac{7}{18}$	$\frac{7}{9}$	$-4. \times 10^{-2}$	1.2×10^{-2}	1.8×10^{-2}	-5.5×10^{-3}	1.1×10^{-2}	3.8×10^{-2}
$\frac{7}{18}$	$\frac{7}{9}$	-2.8×10^{-2}	3.1×10^{-2}	-1.3×10^{-2}	1.4×10^{-2}	-2.9×10^{-2}	-2.6×10^{-2}

$\{\alpha, U, \beta\} = \{0.3, 4.5, 50\}$, AF

q_x/π	q_y/π	N_1^x	N_2^x	N_1^y	N_2^y	N_1^z	N_2^z
-1	1	0	0	-6.1×10^{-2}	0	0	0
1	1	0	0	-6.1×10^{-2}	0	0	0

$\{\alpha, U, \beta\} = \{0.3, 4.75, 50\}$, SI

q_x/π	q_y/π	N_1^x	N_2^x	N_1^y	N_2^y	N_1^z	N_2^z
$\frac{2}{9}$	$\frac{13}{18}$	-5.9×10^{-2}	-3.2×10^{-2}	-1.9×10^{-2}	$-1. \times 10^{-2}$	-2.5×10^{-2}	4.6×10^{-2}
$\frac{13}{18}$	$\frac{2}{9}$	-2.1×10^{-2}	6.2×10^{-3}	-6.4×10^{-2}	1.9×10^{-2}	1.5×10^{-2}	$5. \times 10^{-2}$

$\{\alpha, U, \beta\} = \{0.3, 12.0, 50\}$, SkX

q_x/π	q_y/π	N_1^x	N_2^x	N_1^y	N_2^y	N_1^z	N_2^z
-1	$\frac{1}{3}$	0	0	-2.8×10^{-1}	1.6×10^{-1}	6.9×10^{-2}	1.2×10^{-1}
$-\frac{1}{3}$	1	-2.8×10^{-1}	-1.6×10^{-1}	0	0	6.9×10^{-2}	-1.2×10^{-1}
$\frac{1}{3}$	1	-2.8×10^{-1}	1.6×10^{-1}	0	0	6.9×10^{-2}	1.2×10^{-1}
1	$\frac{1}{3}$	0	0	-2.8×10^{-1}	1.6×10^{-1}	6.9×10^{-2}	1.2×10^{-1}

TABLE IV. Magnetic order parameters $\mathbf{N}_i = (N_i^x, N_i^y, N_i^z)$, $i = 1, 2$ introduced in Eq.(19) and the peak values of $\mathbf{q} = (q_x, q_y)$, together with the parameters $\{\alpha, U, \beta\}$ for phases given in Table II. In the table, we provide the data for magnetic order parameters only for $q_y > 0$, since the values for $q_y < 0$ are related by the inversion symmetry $\mathbf{q} \rightarrow -\mathbf{q}$.